HHS Public Access

Author manuscript

*Clin Cancer Res*. Author manuscript; available in PMC 2018 May 15.

Published in final edited form as:

*Clin Cancer Res*. 2017 May 15; 23(10): 2516–2527. doi:10.1158/1078-0432.CCR-16-1834.

# 5T4-targeted therapy ablates cancer stem cells and prevents recurrence of head and neck squamous cell carcinoma

**Samuel A. Kerk**[1], **Kelsey A. Finkel**[1], **Alexander T. Pearson**[1,2,3], **Kristy A. Warner**[1], **Zhaocheng Zhang**[1], **Felipe Nör**[1,5], **Vivian P. Wagner**[4,5], **Pablo A. Vargas**[6], **Max S. Wicha**[2,3], **Elaine M. Hurt**[7], **Robert E. Hollingsworth**[7], **David A. Tice**[7], and **Jacques E. Nör**[1,3,8,9]

[1]Department of Cariology, Restorative Sciences, Endodontics, University of Michigan School of Dentistry, Ann Arbor, Michigan [2]Department of Internal Medicine, University of Michigan Medical Center, Ann Arbor, Michigan [3]Comprehensive Cancer Center, University of Michigan, Ann Arbor, Michigan [4]Department of Periodontics and Oral Medicine, University of Michigan School of Dentistry, Ann Arbor, Michigan [5]Department of Oral Pathology, Federal University of Rio Grande do Sul, Porto Alegre, Brazil [6]Department of Oral Diagnosis, University of Campinas, Piracicaba, Brazil [7]Oncology Research, MedImmune, Gaithersburg, Maryland [8]Department of Otolaryngology, University of Michigan School of Medicine, Ann Arbor, Michigan [9]Department of Biomedical Engineering, University of Michigan College of Engineering, Ann Arbor, Michigan

## Abstract

**Purpose—**Loco-regional recurrence is a frequent treatment outcome for patients with advanced head and neck squamous cell carcinoma (HNSCC). Emerging evidence suggests that tumor recurrence is mediated by a small subpopulation of uniquely tumorigenic cells, *i.e.* cancer stem cells (CSC), that are resistant to conventional chemotherapy, endowed with self-renewal and multipotency.

**Experimental Design—**Here, we evaluated the efficacy of MEDI0641, a novel antibody-drug conjugate targeted to 5T4 and carrying a DNA-damaging "payload" (pyrrolobenzodiazepine) in preclinical models of HNSCC.

**Results—**Analysis of a tissue microarray containing 77 HNSCC with follow-up of up to 12 years revealed that patients with $5T4^{high}$ tumors displayed lower overall survival than those with $5T4^{low}$ tumors (p=0.038). 5T4 is more highly expressed in head and neck CSC ($ALDH^{high}CD44^{high}$) than in control cells (non-CSC). Treatment with MEDI0641 caused a significant reduction in the CSC fraction in HNSCC cells (UM-SCC-11B, UM-SCC-22B) *in vitro*. Notably, a single intravenous dose of 1 mg/kg MEDI0641 caused long-lasting tumor regression in 3 patient-derived xenograft (PDX) models of HNSCC. MEDI0641 ablated CSC in the PDX-SCC-M0 model, reduced it by 5-fold in the PDX-SCC-M1, and 2-fold in the PDX-SCC-M11 model. Importantly, mice (n=12) treated with neoadjuvant, single administration of MEDI0641 prior to surgical tumor removal

Corresponding author: Jacques E. Nör DDS, PhD, Professor of Dentistry, Otolaryngology, Biomedical Engineering, University of Michigan, 1011 N. University Rm. 2361, Ann Arbor, MI, 48109-1078, United States, Telephone: 734-647-9396, jenor@umich.edu.

**Conflict of interest statement:** David Tice, Elaine Hurt, and Robert Hollingsworth are employees of Medimmune, LLC. Max Wicha is an advisor for and has equity in OncoMed Pharmaceuticals. The remaining authors have no conflicts to declare.

showed no recurrence for over 200 days, while the control group had 7 recurrences (in 12 mice) (p=0.0047).

**Conclusions—**Collectively, these findings demonstrate that an anti-5T4 antibody-drug conjugate reduces the fraction of cancer stem cells and prevents local recurrence, and suggest a novel therapeutic approach for patients with HNSCC.

### Keywords

Tumor initiating cells; Antibody-drug conjugate; Resistance; Progenitor cell targeting; Oral cancer

## Introduction

Head and neck cancer is one of the most common cancers worldwide with 46,000 new cases and 9,000 deaths in the United States each year (1). Head and neck squamous cell carcinoma (HNSCC) is the most common head and neck malignancy, frequently presenting as locally advanced disease (stage III or IVB). The standard of care for HNSCC involves a combination of surgery, radiation, and chemotherapy. Regimens with platinum-based agents such as cisplatin, 5-fluorouracil, or taxanes are frequently administered, along with targeted agents such as the monoclonal anti-EGFR antibody Cetuximab (2). However, despite advances in treatment HNSCC patients still face a 60% risk of local recurrence and 30% risk of distant metastasis. Additionally, patients with recurrent or metastatic tumors typically present enhanced morbidities and poor prognosis, with a median survival time of 10 months (3). It is rather evident that safe, more effective therapies are urgently needed for patients with HNSCC.

The cancer stem cell hypothesis postulates that within a tumor there is a subpopulation of multipotent, tumorigenic cancer stem cells (CSC) capable of reconstituting the heterogeneity of the primary tumor by both self-renewal and differentiation. Cancer stem cells were first isolated in acute myeloid leukemia (AML) and have since been characterized in solid tumors in the breast, brain, lungs, liver, prostate, pancreas, ovaries, kidneys, and colon (4–13). In head and neck cancer, the cancer stem cell fraction shows high activity of the cytosolic enzyme aldehyde dehydrogenase (ALDH), which oxidizes retinoic acid, as well as high expression of the membrane protein CD44 (14,15). Cancer stem cells play an integral role in treatment resistance and disease relapse. As we have shown previously, treatment with cisplatin enhances the cancer stem cell fraction in HNSCC (16). It has been proposed that the slow proliferation rate of cancer stem cells allows them to evade treatments that target highly proliferative cells (17). Further, we observed that Cisplatin enhances the expression of Bmi-1, a key regulator of self-renewal, enabling accumulation of these cells through symmetrical cell division (16). And finally, cancer stem cells present increased expression of ATP-binding cassette (ABC) transporters, which enable them to quickly pump cytotoxic agents out of the cell (18). Collectively, these studies suggest that therapies that target both cancer stem cells and bulk tumor cells would have the potential to induce tumor regression as well as prevent local recurrence and distant disease.

A potential target for such therapies is the oncofetal antigen 5T4, or trophoblast glycoprotein, due to its specificity for cancer tissue and low expression in normal tissue. 5T4

is a 72 kDa, N-glycosylated transmembrane protein whose gene is found on chromosome 6q14-15. Its extracellular domain contains leucine rich repeats (LRR) commonly associated with protein-protein interactions. 5T4 is involved in several cellular functions. It is theorized to play a role in epithelial-to-mesenchymal transition (EMT) as its overexpression correlates with downregulation of E-cadherin (19). 5T4 also mediates CXCL12/CXCR4 signaling (20). The surface expression of 5T4 promotes signaling via CXCR4, which leads to chemotaxis through the MAPK/ERK and PI3K/AKT pathways. In contrast, signaling through CXCR7 in the absence of 5T4 at the plasma membrane causes increased proliferation via EGFR. 5T4 is also involved in modulation in Wnt signaling, as it blocks the internalization of LRP6 and promotes the non-canonical Wnt pathway (21). The potential of oncofetal antigen 5T4 as a cancer stem cell marker has been shown in NSCLC (22). $CD24^{low}CD44^{high}$ cells were found to have increased 5T4 expression. $5T4^{high}$ cells displayed an undifferentiated phenotype as well as increased expression of EMT markers. Sorted $5T4^{high}$ and $5T4^{low}$ cells obtained from patient-derived xenograft (PDX) models of NSCLC were found to have an increased tumorigenic capacity in the $5T4^{high}$ population *in vivo* and reconstituted the original tumor heterogeneity. As a prognostic marker for clinical outcomes, high expression of 5T4 indicates advanced stage disease, potential resistance to treatment, shorter time to recurrence, and poorer overall survival in lung, gastric, ovarian, and colorectal cancer (23–25).

The antibody-drug conjugate (ADC) family of targeted therapies is a promising class of drugs that is designed to deliver cytotoxic chemotherapies specifically to cancer tissues with limited added toxicities. Indeed, when patients with HER2-positive breast cancer were treated with the ADC trastuzumab emtansine *versus* unconjugated lapatinib plus capecitabine, the group receiving the ADC had fewer adverse events and longer overall survival (26). The specificity of oncofetal antigen 5T4 in malignant tissue has been used to develop a novel ADC named MEDI0641 (27). It is targeted to 5T4 and conjugated to the DNA-damaging “payload” pyrrolobenzodiazepine (PBD), which binds to the minor groove of the DNA double helix, hindering its processing. The PBD dimer is released following proteolytic cleavage of the Val-Ala dipeptide, then the low pH in the lysosomal compartment results in self-immolation of the PABA spacer releasing the warhead into the cancer cell. Here, we hypothesized that head and neck cancer stem cells can be eliminated with a 5T4-targeted ADC. Our studies demonstrate that MEDI0641 decreases the cancer stem cell fraction, mediates long-term tumor regression, and prevents tumor recurrence in PDX models of HNSCC.

## Materials and Methods

### Tissue Microarray (TMA)

Cores from paraffin-embedded tumors were prepared by a trained oral pathologist and mounted as a TMA, as described previously (28). Briefly, tumor areas of the invasive front were selected and marked on a hematoxilin-eosin stained slide using an objective marker (Nikon). The slide was then overlaid on the original paraffin block to determine the matching area to be used. Using a manual tissue arrayer (Sakura), 3-D cylindrical cores 2.0 mm in diameter from each tumor were arranged sequentially in a ready-to-use recipient

paraffin block (Sakura). Three cores of normal oral mucosa were inserted into the left upper corner of each recipient block in order to provide orientation. A map specifying the precise position of each case was prepared in order to enable interpretations of staining results. A calibrated observer blinded to all clinical information evaluated the tissue slides. 5T4 staining was evaluated using a conventional light microscope. Each case was evaluated at 100x and 200x magnification regarding protein localization (membranous or membranous/cytosolic), staining intensity (weak, moderate, strong), and percentage of positive cells. The staining intensity was further dichotomized in weak/moderate or strong and the cases were respectively classified as $5T4^{low}$ and $5T4^{high}$.

### Immunohistochemistry

Formalin-fixed, paraffin-embedded tissue sections were deparaffinized in xylene and rehydrated in graded ethanol. Antigen retrieval was carried out in Target Retrieval Solution (Dako). The tissue was permeabilized in 0.1% Triton-x-100 (Sigma) for 20 minutes. Following blocking with Background Sniper (Biocare Medical), tissue sections were exposed to rabbit anti-5T4 (Abcam #134162) at 4°C overnight. Tissue sections were then labeled with MACH3 probe (Biocare Medical), followed by exposure to Horseradish Peroxidase Polymer (Biocare Medical) and visualization with diaminobenzidine (DAB; Biocare Medical).

### *In vivo* studies

Patient-derived xenograft (PDX) tumor models of HNSCC were generated in severe combined immunodeficient (SCID) mice and characterized (29,30). Tumors (PDX-SCC-M0, PDX-SCC-M1, PDX-SCC-M11) were allowed to grow to 200–1000 $mm^3$ and then were treated with either a single dose of 1 mg/kg MEDI0641, a weekly dose of 0.5 mg/kg MEDI0641 for 2 weeks, a weekly dose of 0.33 mg/kg MEDI0641 for 3 weeks, or non-specific IgG1-PBD control. All mouse handling and treatments were performed in under UCUCA-approved protocols.

### Sulforhodamine B (SRB) Assay

The human HNSCC cell lines UM-SCC-11B and UM-SCC-22B (generously provided by Dr. Thomas Carey) were cultured in Dulbecco's Modified Eagle Medium (DMEM; Invitrogen) supplemented with 10% fetal bovine serum (FBS; Invitrogen), and penicillin/streptomycin (Invitrogen). Cells were seeded in quadruplicate wells in 96-well plates (Corning) at a density of 2,000 cells per well. Attached cells were treated with 0–1 μg/mL MEDI0641 or IgG1-PBD control for 24–96 hours. Treated cells were fixed in 50% trichloroacetic acid (Sigma), stained with 0.4% SRB (Sigma), and washed with 1% acetic acid. Bound SRB dye was solubilized in 10 mM Trizma-base. Plates were read in a microplate reader at 560 nm (GENios, Tecan).

### Immunofluorescence

Formalin-fixed, paraffin-embedded tissue sections were deparaffinized in xylene and rehydrated in graded ethanol. Antigen retrieval was carried out in Target Retrieval Solution (Dako). Endogenous peroxidase activity was quenched by incubation in 3% hydrogen

peroxide. Following blocking with Background Sniper (Biocare Medical), tissue sections were exposed to rabbit anti-ALDH (Abcam #52492) or mouse anti-CD44 (Thermo #MS-668-R7). The tissue was then labeled with either mouse or rabbit Alexafluor 488 or 594 (Invitrogen #A11034 or #A11032) and mounted in Vectashield Mounting Medium for Fluorescence with DAPI (Vector Laboratories #H-1200. Alternatively, tissue sections were incubated overnight in TUNEL binding solution (Roche #11684795910). Images were captured with a Nikon Eclipse 80i fluorescence microscope.

## Western blotting

Whole cell lysates were analyzed using SDS-PAGE. Following electrophoresis, proteins were transferred to a nitrocellulose membrane (GE Healthcare Life Sciences) that was blocked in 5% non-fat dry milk and exposed to rabbit anti-5T4 (Abcam #AB134162) or mouse anti-GAPDH (Chemicon International #AB2302). Next, the membranes were washed and exposed to either mouse or rabbit secondary antibody (Jackson Laboratories), incubated in a chemiluminescent solution (Fisher), and exposed to film (Denville).

## Flow Cytometry

Trypsinized cells were filtered through a 40-μm sterile cell strainer (Fisher) and washed with DMEM supplemented with FBS. Alternatively, tumors were harvested from mice, dissociated using the GentleMACS dissociator kit (Miltenyi Biotec), incubated in ACK red blood cell lysis buffer (Invitrogen), and filtered through a 40-μm sterile cell strainer. ALDH activity was quantified using the Aldefluor kit (Stem Cell Tech.) Briefly, single-cell suspensions of $10^6$ cells were incubated in activated Aldefluor substrate (BAAA), or equivalent volume of Aldefluor inhibitor diethyl aminobenzaldehyde (DEAB). CD44 was probed with anti-CD44 (APC #559942, BD Pharmingen or V450 #561292, BD Horizon). 5T4 was probed using MEDI0641 (MedImmune) for 1 hour on ice, followed by labeling with anti-human Alexa Fluor 594 (#A11014; Invitrogen) for 30 minutes at 4°C. Human cells were distinguished by positive anti-HLA-ABC staining (PE #560168; BD Pharmingen), and 7-aminoactinomycin (7AAD #00-6993-50, eBioscience) was used to isolate viable cells. For cell cycle analysis, filtered cells were fixed in 70% ethanol for 1 hour, followed by incubation with propidium iodide (PI #P4864, Sigma) for 30 minutes at 4°C.

## Orosphere Assay

HNSCC cells were sorted for $ALDH^{high}CD44^{high}$ and $ALDH^{low}CD44^{low}$ populations by fluorescence activated cell sorting (FACS), as we described (31). Sorted cells were cultured in DMEM-F12 (Invitrogen) and penicillin/streptomycin (Invitrogen) supplemented with N2 (Invitrogen), rhEGF (Sigma), and FGF (Sigma). Cells were seeded at 2,000 cells per well in 24 well ultra-low attachment plates (Corning). Spheres of 25 cells or more were counted (31). Orospheres were treated with 0–10 μg/ml of MEDI0641 (MedImmune) or IgG1-PBD control (MedImmune) for 24–72 hours.

## Statistical Analysis

Data were analyzed with a one-way analysis of variance (ANOVA) using Prism software (GraphPad Software), and statistical significance was defined as $p<0.05$. To quantify the

univariate relationship between 5T4 expression level and outcomes, we used a log rank test. We used the Cox proportional hazards method for multivariate regression including the following covariates: age, tobacco use, alcohol use, sex, high stage disease, chemotherapy, radiotherapy, surgical resection. The proportional hazards assumption was checked using visual inspection of the scaled Schoenfeld residuals and by testing the Schoenfeld residuals for each covariate versus scaled time. PDX tumor growth data was evaluated from the treatment start time using linear mixed models to incorporate the repeated measurements on each tumor. Model fixed effects included starting tumor size, time, treatment class, and the interaction between time and treatments and model random effects included mouse. A continuous auto-regression correlation structure was employed, which assumes more correlation among temporally proximate observations. Tumor size was log-transformed to account for the exponential growth of tumors. For regression analysis with more than 2 groups, an ANOVA of the model was used to generate the p-value for overall group differences. Analysis was performed using the “nlme” package in the statistical software program R version 3.1.0. For regression analysis between 2 groups, a student’s t-test of the model was used to generate the p-value for differences between the two groups. To assess the relationship between dose and number of orospheres, we used multivariate linear regression. We included dose level, the factor-level day, and the interaction between dose and day. Day was included in our model as a factor. Correlation between ordinal variables was tested using the Spearman’s Rank Correlation Test. Association between categorical variables was tested using a Chi-squared test.

## Results

### 5T4 oncofetal antigen expression correlates with overall survival of patients with HNSCC

We first sought to understand the patterns of expression of 5T4 in HNSCC. A tissue microarray of human HNSCC tumors (n=77) was evaluated for 5T4 staining by a trained oral pathologist blinded for patient outcome. We found that 5T4 is expressed primarily in the cell membrane of tumor cells, with no (or weak) observable staining in the surrounding stromal cells or in normal human oral mucosa control tissue (Fig. 1A). We also observed that high 5T4 expression correlates with shorter overall patient survival (p=0.038) in patients that were followed-up for up to 12 years (Fig. 1B). Using the Chi-squared test we found no significant association between 5T4 expression and gender (p=0.6787), high tobacco use (p=1), or high alcohol consumption (p=0.616). Using Spearman’s correlation test we found no association between 5T4 expression and age (p=0.2735) or clinical stage (p=0.2525) indicating that 5T4 might be considered an independent identifier of patient survival (Fig. 1C).

### MEDI0641 induces long-term tumor regression in PDX models of HNSCC

It has been proposed that low-passage PDX models of cancer recapitulate more accurately the biology human tumors and are valuable tools for preclinical testing of anti-cancer therapies (32). The PDX models used here represent clinical features observed in patients with HNSCC (29,30). Briefly, the PDX-SCC-M0 model was generated from the local recurrence of a patient that was treated with surgery without radiation or chemotherapy. The PDX-SCC-M1 model was generated from the tumor of a previously untreated patient. The

PDX-SCC-M11 model originates from the local recurrence of a tumor in the sinonasal cavity of a patient that was treated with surgery, radiation, and chemotherapy (Docetaxel, Carboplatin, 5-Fluorouracil). These PDX models clearly express 5T4, the target of MEDI0641 (Supplemental Figure 1). Interestingly, we also discovered via immunofluorescence that 5T4 staining co-localizes with CD44, a well-characterized marker of cancer stem cells in HNSCC (15), in the PDX-SCC-M0 model (Supplemental Figure 2).

A single dose of MEDI0641 resulted in complete tumor regression in the PDX-SCC-M0 model for the duration of the experiments, *i.e.* approximately 100–150 days after treatment (Fig. 2A). To determine how robust were the effects of MEDI0641, we allowed the tumors to grow further and then treated two additional PDX models (PDX-SCC-M1, PDX-SCC-M11) with a single injection of the drug. Again, we observed significant regression in tumor volume in these two models. No body weight loss was observed in any of the treatments (Fig. 2A). In the PDX-SCC-M0, PDX-SCC-M1, and PDX-SCC-M11 models, auto-regression correlation analysis of changes in tumor volume following treatment indicated a significant decrease ($p<0.0001$, $p=0.028$, $p=0.033$, respectively) in the MEDI0641-treated groups compared to the group receiving IgG1-PBD control treatment (Fig. 2B).

We next sought to determine the impact of various dosing regimens in the PDX-SCC-M11 model, since it proved to have the least response to a single dose of MEDI0641. All treatment groups received a total dosing of 1 mg/kg MEDI0641, however it was spread out over time in three distinct regimens. Mice were treated with either a single dose of 1 mg/kg MEDI0641; 1 dose every three weeks of 0.5 mg/kg MEDI0641 or IgG1-PBD control (total of 2 doses); or 1 dose every three weeks of 0.33 mg/kg MEDI0641 (total of 3 doses). Linear-regression analysis showed that all three regimens caused a significant reduction ($p<0.0001$) in tumor volume for at least 100 days, as compared to the IgG1-PBD control group. Notably, no significant difference in tumor volume reduction was observed among the three treatment regimens. Again, no body weight loss was observed during treatment (Fig. 2C).

## MEDI0641 induces cell cycle arrest and apoptosis in HNSCC cells

To begin to understand the mechanisms mediating the anti-tumor effect of MEDI0641, we examined the cytotoxic effects of MEDI0641 in established HNSCC cells lines. We first determined the basal 5T4 expression levels in a panel of well-characterized and genotyped HNSCC cell lines (33) (Fig. 3A). Next, we examined the pharmacological effects of MEDI0641 across a range of concentrations and time points. MEDI0641 exhibits low $IC_{50}$ in UM-SCC-11B and UM-SCC-22B cells, which express moderate to high levels of 5T4, with values of 522 ng/ml and 650 ng/ml, respectively, after 72 hours of treatment (Fig. 3B). This is consistent with the values observed by Harper and collaborators in the treatment of breast, gastric, and prostate cancer cells *in vitro* (27). These doses of MEDI0641 induced a $G_2$/M cell cycle arrest, as measured by flow cytometry with propidium iodide, with a maximum effect at 72 hours (Fig. 3C). Notably, we observed an increase in the number of apoptotic cells defined as the sub-$G_0/G_1$ fraction (*i.e.* outside the cell cycle) after treatment with MEDI0641 (Fig. 3C). Interestingly, MEDI0641 had a more modest but still significant effect in two HNSCC cell lines expressing lower levels of 5T4, *i.e.* UM-SCC-14B and UM-SCC-74B (Supplemental Figure 3). Next, we examined PDX-SCC-M11 tissue from mice

that received MEDI0641 (or IgG1-PBD control) to determine if treatment was inducing apoptosis *in vivo* as well. Following *in situ* TUNEL staining, we observed a significant increase ($p<0.0001$) in the number of apoptotic cells in PDX tumors treated with MEDI0641 when compared to IgG1-PBD control (Fig. 3D).

## MEDI0641 decreases the fraction of head and neck cancer stem cells *in vitro*

We next sought to investigate the effect of MEDI0641 on the fraction of head and neck cancer stem cells (*i.e.* $ALDH^{high}CD44^{high}$) in HNSCC cell lines *in vitro* (34). First, we examined the expression of 5T4 in cancer stem cells in UM-SCC-11B and UM-SCC-22B cell lines by flow cytometry. We observed a general trend for increased expression of 5T4 in cancer stem cells when compared to non-cancer stem cells particularly in the UM-SCC-22B cell line ($p=0.0026$) (Fig. 4A). Then, we exposed UM-SCC-11B and UM-SCC-22B cells to MEDI0641 at their respective $IC_{50}$ concentrations. We observed a reduction in the cancer stem cell fraction in UM-SCC-11B from around 35% in cells treated with IgG1-PBD control to 10% in MEDI0641-treated cells ($p=0.03$). In UM-SCC-22B cells, the cancer stem cell fraction was reduced from about 10% to 5% ($p=0.05$) after 72 hours (Fig. 4B).

Culturing HNSCC cells in non-adherent, serum-free conditions selects for cancer stem cells, as we have shown (31). We seeded UM-SCC-22B cells in ultra-low attachment plates, and allowed orospheres to form. Once the orospheres were established, they were treated with increasing doses of MEDI0641 for 24, 48, and 72 hours. We observed a significant overall dose dependence decrease in the number of orospheres per well across all time points ($p=0.0192$) with increasing concentrations of MEDI0641 (Fig. 4C).

## MEDI0641 decreases the fraction of head neck cancer stem cells in PDX HNSCC tumors

We next examined the effect of MEDI0641 on the fraction of cancer stem cells *in vivo*. Mice harboring PDX-SCC-M0, PDX-SCC-M1, or PDX-SCC-M11 tumors were treated with a single dose of either IgG1-PBD control or MEDI0641 and euthanized after 7 days. As expected, mice did not show weight loss and tumor volumes did not decrease significantly as we euthanized mice after a week to determine more accurately the effect of the drug on the fraction of cancer stem cells (Supplemental Figure 4). In the PDX-SCC-M0 model, FACS analysis showed complete ablation of the $ALDH^{high}CD44^{high}$ fraction following treatment, and PDX-SCC-M1 and PDX-SCC-M11 models showed significant decreases ($p=0.0029$ and $p=0.0024$, respectively) (Fig. 5A). Furthermore, this analysis displayed a significant decrease ($p=0.003$) in CD44-positive cells independent of ALDH activity (Supplemental Figure 5). This is perhaps not surprising since CD44 has been shown to be a marker on its own for HNSCC cancer stem cells (15). In addition to flow cytometry, we also studied the effect of MEDI0641 on cancer stem cells by immunofluorescence staining of formalin-fixed, paraffin-embedded PDX tissue. This analysis showed a significant reduction of $ALDH^{high}CD44^{high}$ cells in the MEDI0641 group ($p<0.0001$) as compared to the IgG1-PBD control group (Fig. 5B), confirming the FACS data.

## MEDI0641 prevents local recurrence in PDX models

As cancer stem cells have been implicated in HNSCC dissemination (35), we examined the effect of MEDI0641 in preventing local recurrence *in vivo*. We treated the PDX-SCC-M11

model with either 1 mg/kg IgG1-PBD control or 1 mg/kg MEDI0641 seven days before surgically removing the tumors. The mice were then monitored for tumor recurrence, as defined as a tumor greater than 50 $mm^3$ in the region where the primary tumor was surgically removed. Over the course of 250 days, we observed no recurrences out of 12 mice in the MEDI0641-treated group, while the R347-control group showed recurrences in 7 out of 12 mice ($p=0.0047$) (Fig. 6A). All recurrences were located in the same position as the resected tumor, in the subcutaneous space in the right dorsal region (Fig. 6B). No mice exhibited body weight loss (Fig. 6A). These results were confirmed when we repeated the experiment in an independent experiment ($p=0.011$) (Supplemental Figure 6). Histological analysis of an original and recurrent tumor revealed similar grade, aggressiveness, and morphology as compared to the original tumor in the same mouse (Fig. 6C).

## Discussion

The therapeutic potential of anti-cancer treatments with antibody-drug conjugates depends on target antigens that are highly expressed and specific to tumor cells and on the effectiveness of the cytotoxic “payload”. In this study, we examined the effect of MEDI0641 in preclinical models of HNSCC. A single dose of single agent MEDI0641 caused regression of established PDX HNSCC tumors. Perhaps more importantly, a single dose of MEDI0641 prevented tumor recurrence when used in a neoadjuvant setting prior to surgery. Collectively, these data unveil the therapeutic potential of MEDI0641 in HNSCC, suggesting that patients with these tumors might benefit from treatment with this ADC.

Here, for the first time, we evaluated the expression and prognostic potential of 5T4 in HNSCC. We retroactively analyzed a tissue microarray of 77 patients with HNSCC for 5T4, and observed that patients harboring tumors with high 5T4 expression had lower overall survival as compared to patients with tumors expressing lower 5T4. This result is consistent with previous studies of 5T4 in lung, gastric, ovarian, and colorectal cancer (22–25). Interestingly, in some HNSCC tissue samples, 5T4 was found in the cytosol of the tumor cells in addition to being located in the plasma membrane. The role of 5T4 in tumor cells has not been fully characterized, and further studies regarding the differential expression of 5T4 in the membrane versus the cytosol are warranted. Of note, 5T4 staining in these patient samples was highly specific to cancer cells with very little staining in the surrounding stromal cells, validating the hypothesis that 5T4 oncofetal antigen might be a promising target for antibody-drug conjugate therapy.

We observed that MEDI0641 resulted in long-term tumor regression in PDX models of HNSCC after administering a single dose of MEDI0641 when tumors were already established. The observed tumor regression is likely due to the cytotoxic effect of MEDI0641 to both, cancer stem cells and non-cancer stem cells. Harper and colleagues confirmed this observation in the treatment of breast, gastric, and prostate mouse xenografts as well (28). Indeed, to challenge this therapy we waited until the mean tumor volume reached about 1,000 $mm^3$ in the PDX-SCC-M11 model before injecting MEDI0641. Of note, we selected this model as it represents resistant disease, i.e. this PDX was generated from the recurrence of a patient previously treated with surgery, radiation, and TPF-based chemotherapy. We observed that MEDI0641 caused long-term tumor regression in all PDX

models, regardless of mean tumor volume at treatment initiation. Notably, in the PDX-SCC-M0 model, tumors were ablated completely and did not resume tumor growth for the duration of the study, almost 150 days after a single dose of MEDI0641. Of note, our PDX models exhibited highly variable individual tumor growth rates over time, which is consistent with our previous findings (30). Within a study group, some tumors were considerably larger than others, so if a mouse with a large tumor needed to be euthanized due to protocol requirements, the mean tumor volume for the corresponding group would reflect the loss of that tumor with a sharp decrease in the mean tumor volume calculation. Therefore, we decided to include linear-regression analyses of our raw data to emphasize the fact that MEDI0641 does indeed cause significant tumor regression in all PDX models.

Even though we observed that a single low dose of MEDI0641 was sufficient to induce significant tumor regression, we sought to determine if dividing the same dose over time would affect the efficacy. We divided the study into three treatment regimens, while maintaining the same total dose of 1 mg/kg MEDI0641. We conducted this study in the PDX-SCC-M11 model, since it proved to be the least responsive to treatment in our previous study. After over 200 days of observation, we did not observe any difference in the anti-tumor effect among the three treatment regimens suggesting that the most effective treatment regimen for MEDI0641 is a single injection of the maximum-tolerated dose (MTD). These observations would obviously need to be verified in large animal testing and clinical trials.

While current chemotherapeutic drugs administered in patients with HNSCC are frequently able to de-bulk tumors, it is common for patients to suffer from relapsed disease after treatment is completed. It has been postulated that this might be due to the fact that therapies are not able to eliminate cancer stem cells, which can evade initial treatment and are able to reconstitute the tumor over time (16). We showed here that cancer stem cells express high levels of 5T4 and that MEDI0641 is able to target and reduce the fraction of these cells in both HNSCC cell lines *in vitro* and in all PDX models tested *in vivo*. In fact, in the previously PDX-SCC-M0 model, MEDI0641 completely ablated cancer stem cells. These results might explain why these tumors regressed and did not resume growth after a single injection of MEDI0641.

We next hypothesized that perhaps MEDI0641 would confer protection against local recurrence. For this analysis, we selected model PDX-SCC-M11. The patient from whom the PDX-SCC-M11 model is derived had been previously treated with chemoradiotherapy, and the tumor that was used to generate the PDX model was in fact a recurrent tumor. Indeed, we chose to analyze this model because it had already shown the potential for recurrence in a human patient and we wanted to challenge MEDI0641 with a model of resistant disease. Our hypothesis was proved to be correct, as two independent *in vivo* experiments with this model showed that treatment with MEDI0641 before surgical resection resulted in no local recurrences over a period of up to 200 days. Notably, while the PDX tumors evaluated in these recurrence studies were fairly easily resected from the mouse, HNSCC tumors are notoriously challenging to be surgically removed in humans. Further studies into the effects of MEDI0641, or other 5T4-targeted agents, on local recurrence in HNSCC with considerations for varying scopes of excision are certainly warranted.

Collectively, this work demonstrated that expression of 5T4 oncofetal antigen in the tumor correlates with survival of HNSCC patients, and showed that a single injection of a single agent antibody-drug conjugate targeted to 5T4 is capable of causing regression and preventing recurrence of HNSCC tumors. We attribute these results to the following actions of MEDI0641: A) Ablation of the cancer stem cell population, potentially explaining the capacity of MEDI0641 to prevent tumor regrowth (months after termination of treatment) and to prevent tumor recurrence when used in a neoadjuvant setting; and B) Induction of apoptosis of the more differentiated tumor cells which might explain the capacity of MEDI0641 to causing tumor regression. The remarkable potency and high specificity of MEDI0641 in the work presented here warrant further studies and clinical trials. Indeed, this work suggests that anti-5T4 therapies can potentially become promising treatment options for HNSCC patients.

## Supplementary Material

Refer to Web version on PubMed Central for supplementary material.

## Acknowledgments

**Financial Support:** This work was funded by a grant from MedImmune through the MedImmune-University of Michigan Agreement; University of Michigan Head Neck SPORE P50-CA97248 from the NIH/NCI; and grant R01-DE21139 from the NIH/NIDCR (JEN)

We thank the patients who kindly provided the tumor specimens used to generate the patient-derived xenograft (PDX) models needed for this research. We also thank the surgeons, nurses and support staff that enabled the process of tumor specimen collection and processing for use in research. We also thank Dr. Thomas Carey for providing us with the UM-SCC-11B and UM-SCC-22B cell lines. We would like to sincerely thank the members of the University of Michigan Flow and Histology Cores for their assistance with experimental design and data processing.

## References

1. Siegel RL, Miller KD, Jemal A. Cancer statistics, 2016. CA Cancer J Clin. 2016; 66:7–30. [PubMed: 26742998]
2. Seiwert TY, Cohen EEW. State-of-the-art management of locally advanced head and neck cancer. Br J Cancer. 2005; 92:1341–8. [PubMed: 15846296]
3. Sacco GA, Cohen EE. Current treatment options for recurrent or metastatic head and neck squamous cell carcinoma. J Clin Oncol. 2015; 33:3305–13. [PubMed: 26351341]
4. Lapidot T, Sirard C, Vormoor J, et al. A cell initiating human acute myeloid leukaemia after transplantation into SCID mice. Nature. 1994; 367:645–8. [PubMed: 7509044]
5. Al-Hajj M, Wicha MS, Benito-Hernandez A, Morrison SJ, Clarke MF. Prospective identification of tumorigenic breast cancer cells. Proc Natl Acad Sci US A. 2003; 100:3983–8.
6. Singh SK, Clarke ID, Terasaki M, Bonn VE, Hawkins C, Squire J, et al. Identification of a cancer stem cell in human brain tumors. Cancer Res. 2003; 63:5821–8. [PubMed: 14522905]
7. Eramo A, Lotti F, Sette G, Pilozzi E, Biffoni M, Di Virgilio A, et al. Identification and expansion of the tumorigenic lung cancer stem cell population. Cell Death Differ. 2008; 15:504–14. [PubMed: 18049477]
8. Ma S, Chan KW, Hu L, Lee TK, Wo JY, Ng IO, et al. Identification and characterization of tumorigenic liver cancer stem/progenitor cells. Gastroenterology. 2007; 132:2542–56. [PubMed: 17570225]
9. Collins AT, Berry PA, Hyde C, Stower MJ, Maitland NJ. Prospective identification of tumorigenic prostate cancer stem cells. Cancer Res. 2005; 65:10946–51. [PubMed: 16322242]

10. Hermann PC, Huber SL, Herrler T, Aicher A, Ellwart JW, Guba M, et al. Distinct populations of cancer stem cells determine tumor growth and metastatic activity in human pancreatic cancer. Cell Stem Cell. 2007; 1:313–23. [PubMed: 18371365]
11. Bapat SA, Mali AM, Koppikar CB, Kurrey NK. Stem and progenitor-like cells contribute to the aggressive behavior of human epithelial ovarian cancer. Cancer Res. 2005; 65:3025–9. [PubMed: 15833827]
12. Bussolati B, Bruno S, Grange C, Buttiglieri S, Deregibus MC, Cantino D, et al. Isolation of renal progenitor cells from adult human kidney. Am J Pathol. 2005; 166:545–55. [PubMed: 15681837]
13. O'Brien CA, Pollett A, Gallinger S, Dick JE. A human colon cancer cell capable of initiating tumour growth in immunodeficient mice. Nature. 2007; 445:106–10. [PubMed: 17122772]
14. Clay MR, Tabor M, Owen JH, Carey TE, Bradford CR, Wolf GT, et al. Single-marker identification of head and neck squamous cell carcinoma cancer stem cells with aldehyde dehydrogenase. Head Neck. 2010; 32:1195–201. [PubMed: 20073073]
15. Prince ME, Sivanandan R, Kaczorowski A, Wolf GT, Kaplan MJ, Dalerba P, et al. Identification of a subpopulation of cells with cancer stem cell properties in head and neck squamous cell carcinoma. Proc Natl Acad Sci US A. 2007; 104:973–978.
16. Nör C, Zhang Z, Warner KA, Bernardi L, Visioli F, Helman JI, et al. Cisplatin induces Bmi-1 and enhances the stem cell fraction in head and neck cancer. Neoplasia. 2014; 16:137–46. [PubMed: 24709421]
17. Moore N, Lyle S. Quiescent, slow-cycling stem cell populations in cancer: a review of the evidence and discussion of significance. J Oncol. 2011; 2011:396076. [PubMed: 20936110]
18. Zhou S, Schuetz JD, Bunting KD, Colapietro AM, Sampath J, Morris JJ, et al. The ABC transporter Bcrp1/ABCG2 is expressed in a wide variety of stem cells and is a molecular determinant of the side-population phenotype. Nat Med. 2001; 7:1028–34. [PubMed: 11533706]
19. Spencer HL, Eastham AM, Merry CL, Southgate TD, Perez-Campo F, Soncin F, et al. E-cadherin inhibits cell surface localization of the pro-migratory 5T4 oncofetal antigen in mouse embryonic stem cells. Mol Biol Cell. 2007; 18:2838–51. [PubMed: 17507657]
20. Southgate TD, McGinn OJ, Castro FV, Rutkowski AJ, Al-Muftah M, Marinov G, et al. CXCR4 mediated chemotaxis is regulated by 5T4 oncofetal glycoprotein in mouse embryonic cells. PLoS One. 2010; 5:e9982. [PubMed: 20376365]
21. Stern PL, Brazzatti J, Sawan S, McGinn OJ. Understanding and exploiting 5T4 oncofoetal glycoprotein expression. Semin Cancer Biol. 2014; 29:13–20. [PubMed: 25066861]
22. Damelin M, Geles KG, Follettie MT, Yuan P, Baxter M, Golas J, et al. Delineation of a cellular hierarchy in lung cancer reveals an oncofetal antigen expressed on tumor-initiating cells. Cancer Res. 2011; 71:4236–46. [PubMed: 21540235]
23. Naganuma H, Kono K, Mori Y, Takayoshi S, Stern PL, Tasaka K, et al. Oncofetal antigen 5T4 as a prognostic factor in patients with gastric cancer. Anticancer Res. 2002; 22:1033–8. [PubMed: 12168897]
24. Wrigley E, McGown AT, Rennison J, Swindell R, Crowther D, Starzynska T, et al. 5T4 oncofetal antigen expression in ovarian carcinoma. Int J Gynecol Cancer. 1995; 5:269–74. [PubMed: 11578488]
25. Starzynska T, Marsh PJ, Schofield PF, Roberts SA, Myers KA, Stern PL. Prognostic significance of 5T4 oncofetal antigen in colorectal carcinoma. Br J Cancer. 1994; 69:899–902. [PubMed: 8180020]
26. Verma S, Miles D, Gianni L, Krop IE, Welslau M, Baselga J, et al. Trastuzumab emtansine for HER2-positive advanced breast cancer. New Engl J Med. 2012; 367:1783–91. [PubMed: 23020162]
27. Harper J, Lloyd C, Dimasi N, Toader D, Marwood R, Lewis L, et al. Evaluation of antibody-drug conjugate (ADC) payloads with different mechanisms of action reveals a pyrrolobenzodiazepine-conjugated ADC targeting 5T4 with potent anti-cancer stem cell activity. Cancer Res. (submitted).
28. Fonseca FB, de Andrade BA, Rangel AL, Della Coletta R, Lopes MA, de Almeida OP, et al. Tissue microarray is a reliable method for immunohistochemical analysis of pleomorphic adenoma. Oral Surg Oral Med Oral Pathol Oral Radiol. 2014; 117:81–8. [PubMed: 24332331]

29. Finkel KA, Warner KA, Bradford CR, McLean SA, Prince ME, Zhong H, et al. IL-6 inhibition with MEDI5117 decreases the fraction of head and neck cancer stem cells and prevents tumor recurrence. Neoplasia. 2016; 18:273–81. [PubMed: 27237319]

30. Pearson AT, Finkel KA, Warner KA, Nor F, Tice D, Martins MD, et al. Patient-derived xenograft (PDX) tumors increase growth rate with time. Oncotarget. 2016; 7:7993–8005. [PubMed: 26783960]

31. Krishnamurthy S, Nör JE. Orosphere Assay: A method for propagation of head and neck cancer stem cells. Head Neck. 2013; 35:1015–21. [PubMed: 22791367]

32. Hidalgo M, Amant F, Biankin AV, Budinska E, Byrne AT, Caldas C, et al. Patient-derived xenograft models: an emerging platform for translational cancer research. Cancer Discov. 2014; 4:998–1013. [PubMed: 25185190]

33. Brenner JC, Graham MP, Kumar B, Saunders LM, Kupfer R, Lyons RH, et al. Genotyping of 73 UM-SCC head and neck squamous cell carcinoma cell lines. Head Neck. 2010; 32(4):417–26. [PubMed: 19760794]

34. Krishnamurthy S, Dong Z, Vodopyanov D, Imai A, Helman JI, Prince ME, Wicha MS, Nör JE. Endothelial cell-initiated signaling promotes the survival and self-renewal of cancer stem cells. Cancer Res. 2010; 70:9969–78. [PubMed: 21098716]

35. Chinn SB, Darr OA, Owen JH, Bellile E, McHugh JB, Spector ME, et al. Cancer stem cells: mediators of tumorigenesis and metastasis in head and neck squamous cell carcinoma. Head Neck. 2015; 37:317–26. [PubMed: 24415402]

## Translational Relevance

Head and neck cancer is a common and deadly malignancy that is generally treated with surgical resection, platinum-based chemotherapy, and radiation. Current standard-of-care treatment typically results in high morbidity for these patients, and disease relapse is rather common. Emerging evidence suggests that the recurrence and metastases of these tumors are mediated by cancer stem cells. Here, we showed that a transmembrane glycoprotein (5T4 oncofetal antigen) is expressed primarily by head and neck squamous cell carcinoma (HNSCC) cells, particularly by cancer stem cells, and that 5T4 expression correlates negatively with overall patient survival. We also demonstrated that MEDI0641, a novel antibody-drug conjugate targeted to 5T4, mediates the regression of patient-derived xenograft (PDX) tumors, reduces the fraction of cancer stem cells, and prevents local recurrence. Collectively, these data suggest that patients with head and neck cancer might benefit from therapeutic ablation of 5T4-positive cells.

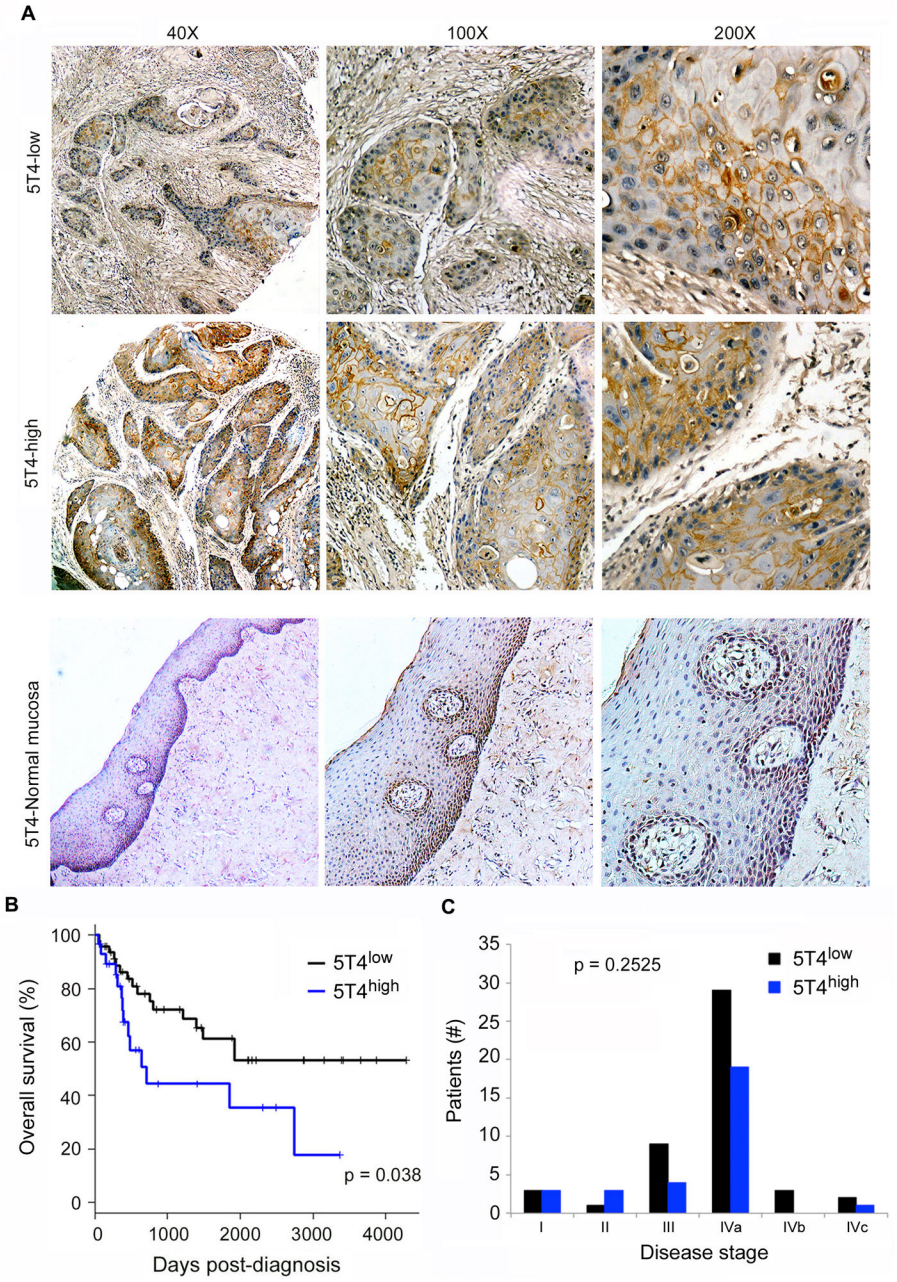


**Figure 1.**

5T4 oncofetal antigen is expressed in HNSCC and correlates with overall survival. **(A)** Immunohistochemistry staining for 5T4 in human HNSCC tumor cores. Images are representative of staining patterns in 5T4-low and 5T4-high groups, as well as 5T4 expression in normal human oral mucosa control tissue. **(B)** Graph depicting overall survival over time in tumors with high and low 5T4 expression. **(C)** Graph depicting the breakdown of 5T4-low and 5T4-high tumors by disease stage at time of diagnosis.

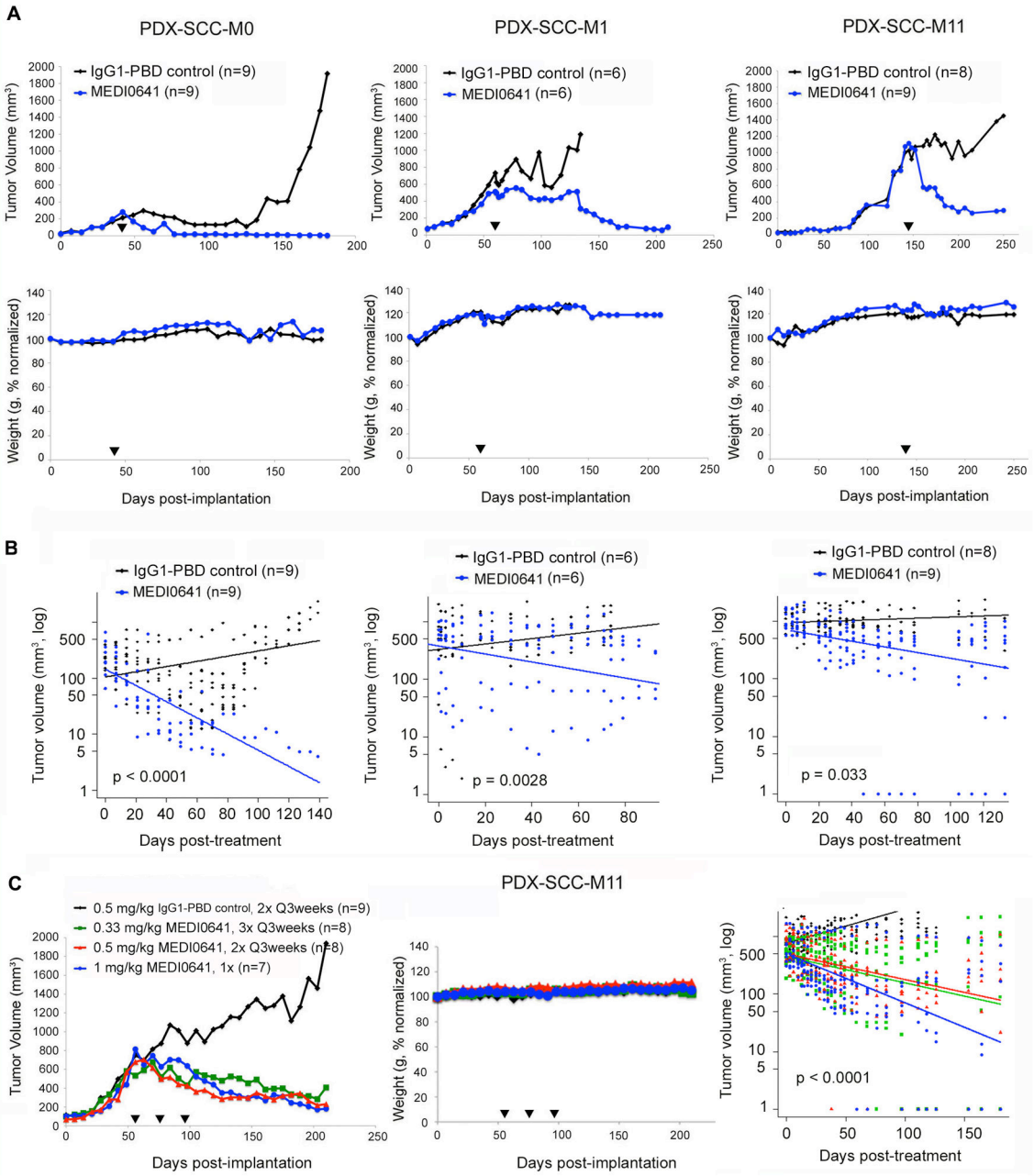


**Figure 2.**

MEDI0641 induces long-term tumor regression in PDX models of HNSCC. **(A)** Graphs depicting mean tumor volume and normalized weight over time in the PDX-SCC-M0, PDX-SCC-M1, and PDX-SCC-M11 models after treatment with a single dose of MEDI0641 or IgG1-PBD control. Mice received 0.33 mg/kg MEDI0641 or IgG1-PBD control in the experiment performed with PDX-SCC-M0 tumors, or 1 mg/kg MEDI0641 or IgG1-PBD control in the experiment with PDX-SCC-M1 and PDX-SCC-M11 tumors. Black arrows indicate when MEDI0641 was administered. **(B)** Graphs depicting auto-regression analyses of data acquired in the PDX-SCC-M0, PDX-SCC-M1, and PDX-SCC-M11 models from

experiments performed in panel A. Data for these graphs were analyzed only post-treatment. Please note the y-axes are on a log scale. **(C)** Graphs depicting mean tumor volume, normalized weight, and auto-regression analysis in the PDX-SCC-M11 model over time after receiving various dosing regimens of MEDI0641. Black arrows represent treatment initiation. Auto-regression analysis was only generated for data post-treatment, as in panel B. Please again take note of the log scale y-axis.

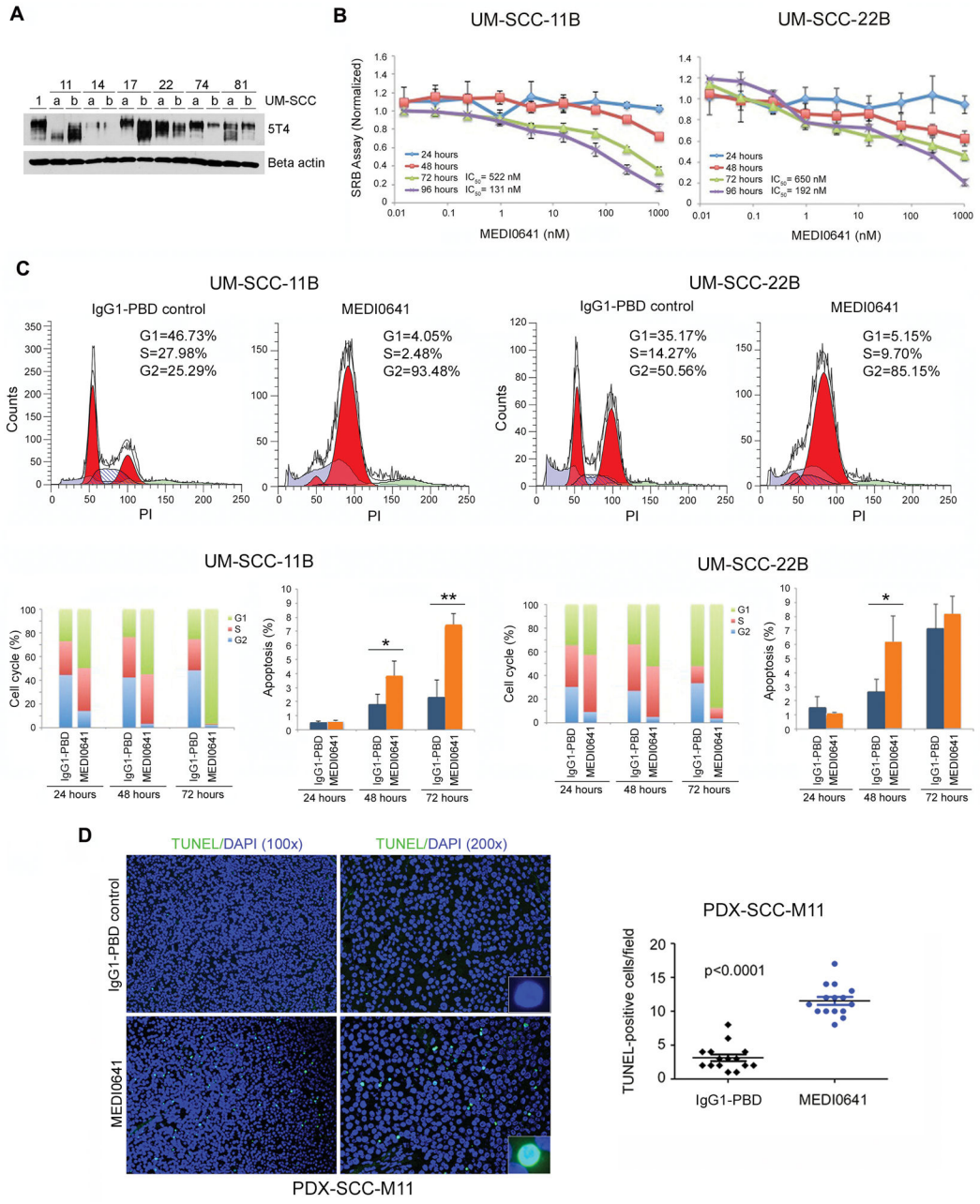


**Figure 3.**

MEDI0641 induces G2/M cell cycle arrest and induces apoptosis. **(A)** Western blot showing the endogenous expression of 5T4 oncofetal antigen in a panel of HNSCC cell lines. **(B)** Graphs of SRB assays in UM-SCC-11B and UM-SCC-22B cells depicting optical density at 565 nm normalized to IgG1-PBD control over increasing concentrations of MEDI0641 at 24, 48, 72, and 96 hours. **(C)** Modfit depictions of cell cycle changes in UM-SCC-11B and UM-SCC-22B cells following treatment with 521 ng/mL and 686 ng/mL, respectively, of either IgG1-PBD control or MEDI0641 at 72 hours. Graphs depicting triplicate analyses of the changes in cell cycle and apoptosis in UM-SCC-11Bs and UM-SCC-22Bs at 24, 48, and

72 hours. *p<0.05, **p<0.005. **(D)** Representative images (200x) of TUNEL staining for apoptosis in PDX-SCC-M11 tissue samples treated with a single dose of 1 mg/kg MEDI0641 or control 1 mg/kg IgG1-PBD 7 days prior to euthanasia. Inserts are at 400x magnification. Pictures were taken of five fields per tumor in three tumors per group. A graph depicting TUNEL-positive cells per field in the control IgG1-PBD and MEDI0641 treatment groups.

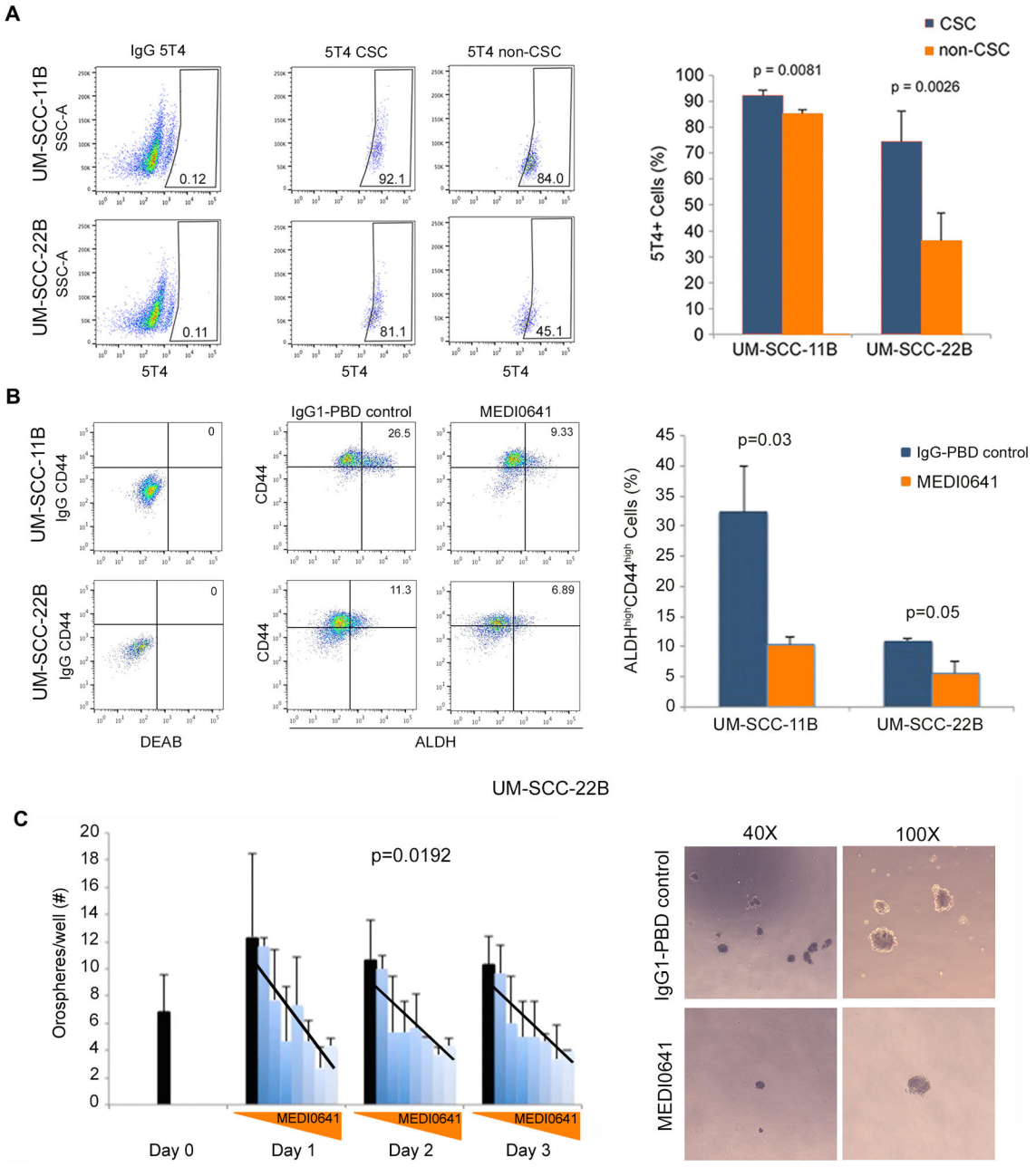


**Figure 4.**

5T4 is highly expressed in CSCs and MEDI0641 targets these cells in normal and low-attachment conditions. **(A)** Flow cytometry gating and graph depicting the expression of 5T4 in the CSC and non-CSC fractions in UM-SCC-11B and UM-SCC-22B cells. **(B)** Flow cytometry gating and graph depicting the percentage of $ALDH^{high}CD44^{high}$ cells in UM-SCC-11B and UM-SCC-22B cells following treatment with the $IC_{50}$ values for each line (522 ng/mL or 686 ng/mL, respectively) of either IgG1-PBD control or MEDI0641. **(C)** Graph depicting the number of UM-SCC-22B orospheres per well over time after treatment with a 2-fold concentration gradient of MEDI0641 at 0.156, 0.312, 0.625, 1.25, 2.5, 5, and

10 μg/mL. IgG1-PBD control treatments represented by the solid black bars, were given at 10 μg/mL. Superimposed lines were generated from regression analyses of dose dependency at each time point. Representative images of orospheres after 3 days of treatment with either 10 μg/mL IgG1-PBD control or MEDI0641 at 40x and 100x magnifications.

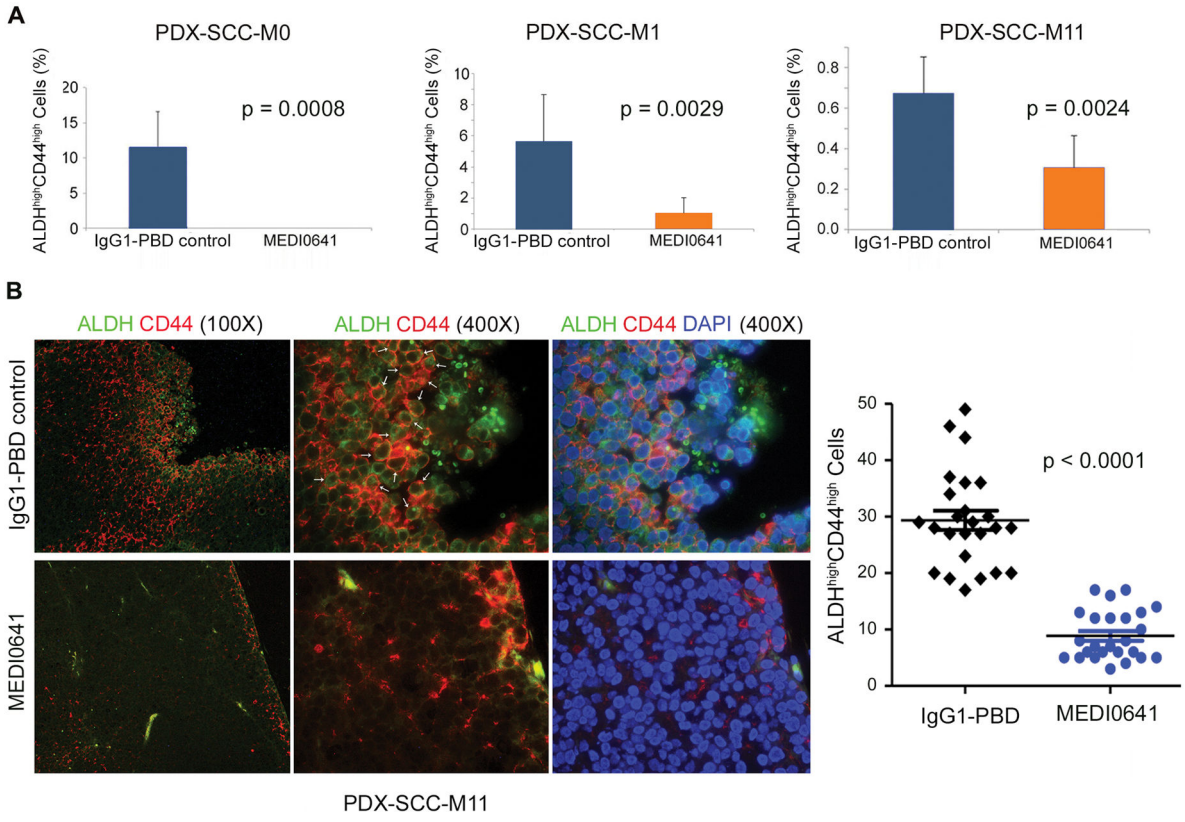


**Figure 5.**

MEDI0641 reduces the CSC fraction in PDX models of HNSCC. **(A)** Graphs depicting the percentage of ALDH$^{high}$CD44$^{high}$ cells in the PDX-SCC-M0, PDX-SCC-M1, and PDX-SCC-M11 models after treatment with either IgG1-PBD control or MEDI0641 (0.33 mg/kg PDX-SCC-M0 model, 1.0 mg/kg PDX-SCC-M1 and PDX-SCC-M11 models). **(B)** Representative images of immunofluorescent staining in PDX-SCC-M11 tissue treated with either 1.0 mg/kg MEDI0641 or IgG1-PBD control. Cytosolic ALDH is green, membrane CD44 is red, and nuclear DAPI is blue. White arrows indicate examples of cells with both ALDH and CD44 staining. A graph depicting the quantification of ALDH$^{high}$CD44$^{high}$ cells in tumors treated with 1.0 mg/kg MEDI0641 or IgG1-PBD control. Five tumors and five fields per tumor were analyzed for both groups.

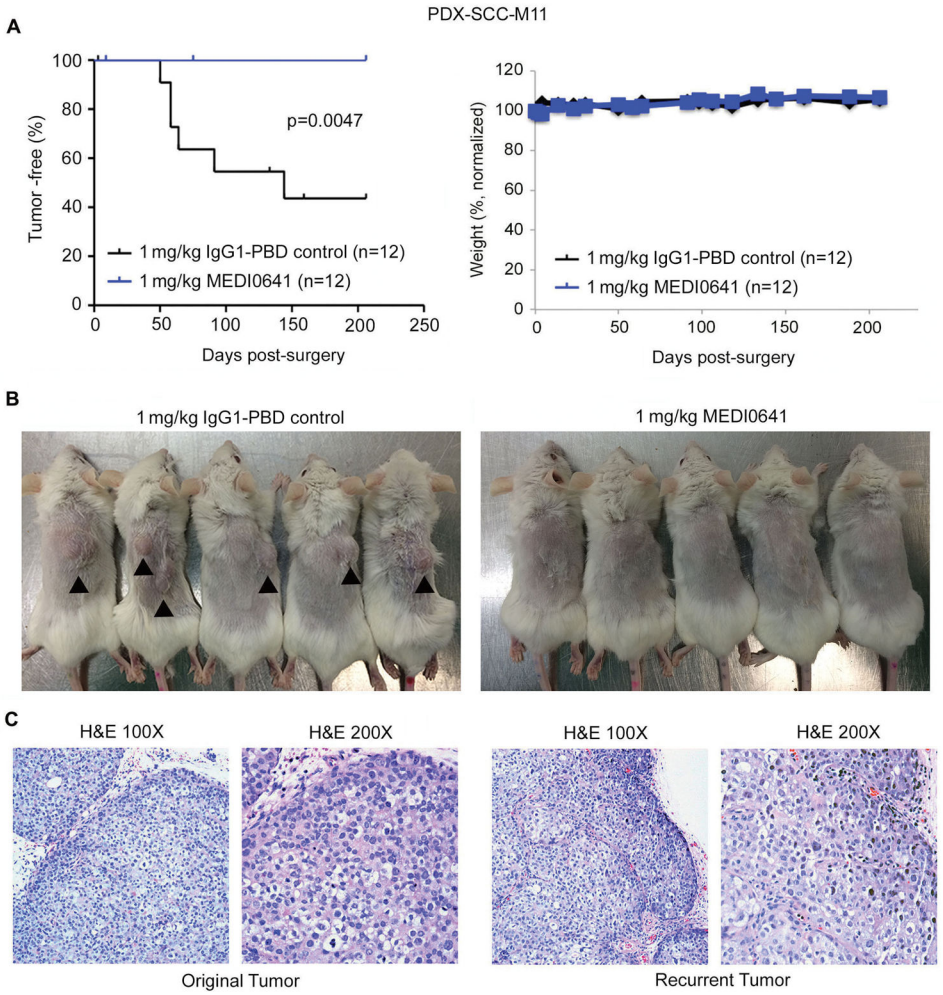


**Figure 6.**

MEDI0641 prevents local recurrence after surgical resection in a PDX model. **(A)** A Kaplan-Meier graph depicting incidences of local recurrence following surgery in the PDX-SCC-M11 model after treatment with either 1 mg/kg MEDI0641 or IgG1-PBD control over time. A graph depicting the mean normalized weight of mice in both groups following surgery. **(B)** Images showing incidences of local recurrence in IgG1-PBD control mice and images showing a lack of local recurrences in MEDI0641 mice. Black arrows indicate recurrent tumors. **(C)** H&E images of an original PDX-SCC-M11 PDX tumor compared to an PDX-SCC-M11 recurrent tumor.